ECS Journal of Solid State
Science and Technology

Editors' Choice—Growth of Layered WS_2 Electrocatalysts for Highly Efficient Hydrogen Production Reaction

JSS Focus Issue on Properties, Devices, and Applications Based on 2D Layered Materials

Growth of Layered WS_2 Electrocatalysts for Highly Efficient Hydrogen Production Reaction

Merfat M. Alsabban,[a,b,c] Shixiong Min,[a,b,d] M. N. Hedhili,[a] Jun Ming,[a] Lain-Jong Li,[a,*] and Kuo-Wei Huang[a,b,z]

[a]*Physical Sciences and Engineering, King Abdullah University of Science and Technology, Thuwal 23955-6900, Kingdom of Saudi Arabia*
[b]*KAUST Catalysis Center, King Abdullah University of Science and Technology, Thuwal 23955-6900, Kingdom of Saudi Arabia*
[c]*Department of Chemistry, King Abdulaziz University, Jeddah 21589, Kingdom of Saudi Arabia*
[d]*School of Chemistry and Chemical Engineering, Beifang University of Nationalities, Yinchuan 750021, People's Republic of China*

Seeking more economical alternative electrocatalysts without sacrificing much in performance to replace precious metal Pt is one of the major research topics in hydrogen evolution reactions (HER). Tungsten disulfide (WS_2) has been recognized as a promising substitute for Pt owing to its high efficiency and low-cost. Since most existing works adopt solution-synthesized WS_2 crystallites for HER, direct growth of WS_2 layered materials on conducting substrates should offer new opportunities. The growth of WS_2 by the thermolysis of ammonium tetrathiotungstate $(NH_4)_2WS_4$ was examined under various gaseous environments. Structural analysis and electrochemical studies show that the H_2S environment leads to the WS_2 catalysts with superior HER performance with an extremely low overpotential ($\eta_{10} = 184$ mV).

Manuscript submitted June 28, 2016; revised manuscript received August 1, 2016. Published August 17, 2016. *This paper is part of the JSS Focus Issue on Properties, Devices, and Applications Based on 2D Layered Materials.*

The future economy requires the production of clean energy to replace fossil fuels. Hydrogen is considered as one of the promising future options as a pollution-free energy carrier. Practically, electrocatalytic water splitting has gained attention for sustainable hydrogen production.[1] Accordingly, scientists are eagerly seeking for an electrocatalyst that could act as an alternative to the most electrochemically active but expensive platinum metal.[2–4] Tungsten disulfide, WS_2, a member of the semiconducting transition metal dichalcogenide family, has drawn considerable attention due to its semiconducting nature and electrocatalytic activities.[5–8] Nevertheless, very few studies have been conducted on WS_2 regarding to HER up to date.[5,9–11] The systematic studies of layered WS_2 materials for HER are still not available.[1] Herein, we report our preparation of layered WS_2 electrocatalysts for highly efficient hydrogen production reaction.

We have performed the growth of WS_2 by the thermolysis of ammonium tetrathiotungstate $(NH_4)_2WS_4$ on conducting carbon cloth (CC) substrates under different gaseous environments. As CC is conducting with a high surface area, it is an ideal substrate for loading the WS_2 materials.[1] The influence of environmental gas on the electrochemical activity of the obtained WS_2 catalysts were studied. H_2S was found to give the WS_2 electrocatalysts with superior performance for the hydrogen production with a current density of 10 mA cm^{-2} at a low overpotential of 184 mV.

Materials and Methods

Materials.—All chemicals including sulfuric acid (H_2SO_4) and ammonium tetrathiotungstate $(NH_4)_2WS_4$ were purchased from commercial sources and used without further purification. Water used was purified through a Millipore system.

Preparation of WS_2.—The precursor, ammonium tetrathiotungstate solution ($(NH_4)_2WS_4$ (Alfa Aesa 99.9%) in 5.0 wt% in DMF (dimethylformamide)), was casted on CC substrates (W0S1002 from CeTech) with a loading amount of 1 mg/cm^2 (Scheme 1). The drop-casted conducting carbon cloth substrate was then baked on a hot plate at 160°C for 20 min. Subsequently, it was fed into the tube furnace for thermolysis process under atmospheric pressure (AP) at varied temperatures and in different gaseous environments, including H_2S and Ar (10 and 90 sccm respectively), H_2 and Ar (10 and 90 sccm respectively), and pure Ar (100 sccm). In order to exclude oxygen species from the system, tube furnace was pumped and purged with Ar before switching to different gas.

Characterizations.—The surface morphology of the catalysts was observed by field-emission scanning electron microscopy (FESEM, FEI Quanta 600). X-ray diffraction (XRD, Bruker D8 Discover diffractometer, using Cu Kα radiation, $\lambda = 1.540598$ Å) was used to investigate the crystalline structure. XPS studies were carried out in a Kratos Axis Ultra DLD spectrometer equipped with a monochromatic Al Kα X-ray source ($h\nu = 1486.6$ eV) operating at 150 W, a multi-channel plate and delay line detector under 1.0×10^{-9} torr vacuum. Measurements were performed in hybrid mode using electrostatic and magnetic lenses, and the take-off angle (angle between the sample surface normal and the electron optical axis of the spectrometer) was 0°. All spectra were recorded using an aperture slot of 300 μm × 700 μm. The survey and high-resolution spectra were collected at fixed analyzer pass energies of 160 and 20 eV, respectively. Samples were mounted in floating mode in order to avoid differential charging.[12] Charge neutralization was required for all samples. Binding energies were referenced to the C 1s peak (set at 284.4 eV) of the sp^2 hybridized (C=C) carbon from the carbon cloth substrate. The data were analyzed with commercially available software, CasaXPS. The individual peaks were fitted by a Gaussian (70%)–Lorentzian (30%) (GL30) function after linear or Shirley type background subtraction. Raman spectrometer LabRAMAramis (HoribaJobinYvon) was used in a range of 100–3500 cm^{-1}. The spectra were detected by a diode-pumped solid state (DPSS) laser at room temperature with 473 nm wavelength acting as the excitation source. Additionally, a microscope (Olympus BX 41) with a total of 1006 objective lens was

*Electrochemical Society Member.
[z]E-mail: hkw@kaust.edu.sa

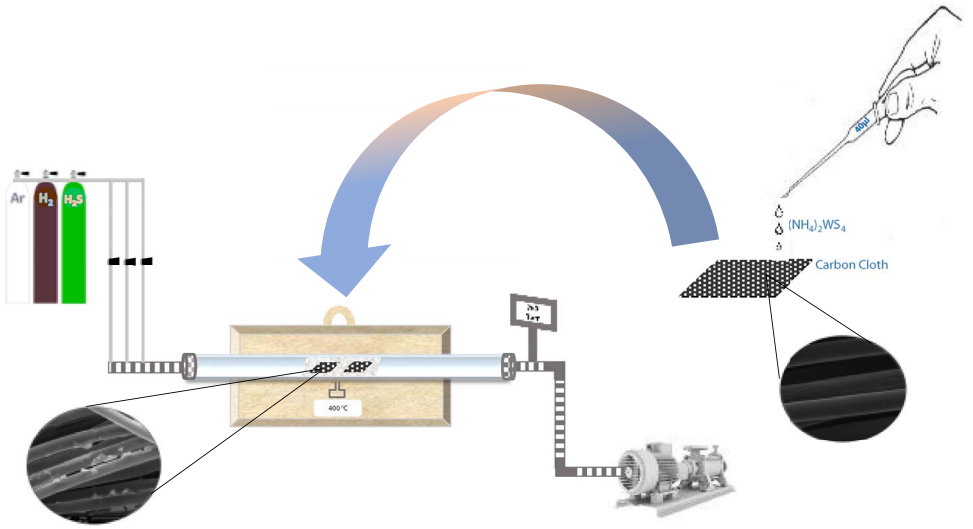

Scheme 1. Schematic representation of the growth of WS_2 on CC. The $(NH_4)_2WS_4$ solution was drop-casted on CC, followed by drying on a hot-plate. The loaded carbon cloth was fed into tube furnace for thermolysis process at various temperatures and gaseous environments.

used to focus incident laser beam to a spot of 1 μm diameter. And for calibration, Si peak at 521 cm^{-1} was used.

Electrochemical measurements.—All electrochemical measurements were performed at room temperature in a PGSTAT 302N Autolab potentiostat/galvanostat (Metrohm). The hydrogen evolution reaction performance of WS_2 was assessed by measuring polarization curves with linear sweep voltammetry (LSV) with a scan rate of 0.5 mV/s. In the 0.5 M H_2SO_4 (pH = 0.34) solution, Nernst equation becomes E(RHE) = E(Ag/AgCl) + 0.228. A separate RHE calibration in a hydrogen saturated electrolyte has been accomplished with 0.225 V offset, which perfectly coincides with 0.228 in the equation. Instead of Pt anode, which may dissolve during the reaction into the electrolyte and contaminate our catalytic cathode, graphite rod was used as a counter electrode, while Ag/AgCl (in 3 M KCl solution) electrode used as a reference electrode.

Results and Discussion

Spectroscopic characterizations of WS_2.—The microstructure of the electrocatalysts was examined using scanning electron microscopy (SEM). Figure 1 shows the surface morphology of WS_2/CC after calcination to 400°C in a H_2S/Ar environment. It is clearly shown that WS_2 forms a uniform thin layer on the fibers of carbon cloth.

To gain a better insight into the composition and crystalline structure of our materials, alongside with confirmation of the identity of the final product, X-ray diffraction (XRD) analysis was performed. Figure 2a displays the XRD patterns of the WS_2/CC annealed at 400°C and acquired under different gaseous environments, H_2S, H_2, and Ar. The peaks at 2θ = 26.1°, 43.3° and 53.8° from carbon cloth are marked as "C". Regardless of various annealing environments, two obvious reflection peaks at 14.3° and 59.4°, assigned to (002) and (110) crystalline orientations of WS_2, can always be observed.

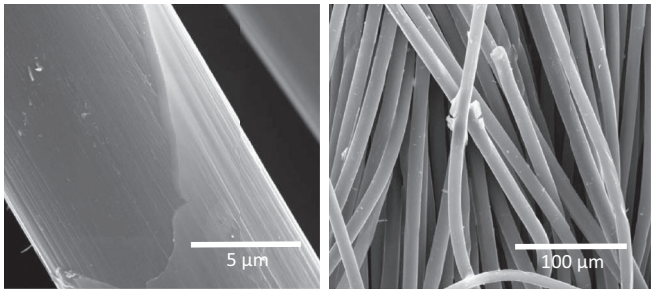

Figure 1. SEM images of carbon cloth loaded with WS_2 at 400°C–10% H_2S/90%Ar environment.

The Raman spectra in Figure 2e also indicates that there is no pronounced difference in their vibration modes E_{1g}, $E^1{}_{2g}$, and A_{1g} detected at 294.6 cm^{-1}, 351.2 cm^{-1}, and 416.3 cm^{-1}, respectively. These results suggest that the crystal structures of WS_2 formulated by thermolysis of $(NH_4)_2WS_4$ are similar in spite of the different gas environments. Unexpectedly, and in spite of pumping the furnace tube to remove the oxygen species, WO_3 peak at 2θ was still detected at 33.5°. These oxides are formed due to the presence of unavoidable trace amount of oxygen in the system, which may react with $(NH_4)_2WS_4$ precursor and yield WO_3.

Since the catalytic reactions are known to occur on the surface of the catalysts, it is more informative to probe the surface bonding structures. In this respect, XPS study is a better methodology. We first studied the W 4f and S 2p core levels of the WS_2 annealed at different temperatures 200°C, 400°C and 800°C in the presence of H_2S gas (Figures 3a and 3b). The W 4f region was decomposed into three doublets (W $4f_{7/2}$ – W $4f_{5/2}$) with a fixed area ratio equal to 4:3 and doublet separation of 2.14 eV and a singlet W $4p_{5/2}$. The binding energies of W $4f_{7/2}$ for the three components are 32.7 eV, 33.5 eV, and 36.1 eV. While binding energy of the singlet W $4p_{5/2}$ is at 38.5 eV. The W $4f_{7/2}$ component at 32.7 eV is attributed to prismatic 2H-WS_2, whereas the W $4f_{7/2}$ component at 36.1 eV corresponds to WO_3.[1,13–18] The W $4f_{7/2}$ component at 33.5 eV is attributed to oxy-sulfide intermediate phase denoted WO_xS_y.[15,16,18] The most probable oxy-sulfide intermediate phase is WOS_2.[19] The S 2p level was fitted with four spin-orbit doublets (S $2p_{3/2}$–S $2p_{1/2}$) with fixed area ratio equal to 2:1 and doublet separation at 1.18 eV. The S $2p_{3/2}$ components were located at the binding energy values of 161.1, 162.3, 163.5–163.7 and 168–169 eV, respectively. The dominant S $2p_{3/2}$ component centered at 162.3 eV corresponds to sulfur S^{2-} in 2H-WS_2.[1,14–17] The component at 163.5–163.7 eV is attributed to disulfide pairs $S_2{}^{2-}$ in a mixed oxygen-sulfur environment[15] and/or to bridging disulfide ligands $S_2{}^{2-}$ and apical S^{2-} from WS_3 phase.[1,20,21] Both WS_2 and WS_3 contain W^{4+} and S^{2-} species; however, only WS_3 possess the $S_2{}^{2-}$ ligand,[19] with a formal charge state of $[W^{4+}(S_2{}^{2-})(S^{2-})]$.[22] The component at 161.1 eV is attributed to sulfur ions of S^{2-} type with more negative real charge.[15] The component located at 168–169 eV is assigned oxidized sulfur species.[23]

The precursor, ammonium tetrathiotungstate solution $(NH_4)_2WS_4$, is dissolved in solvent and it has to go through a preliminary baking

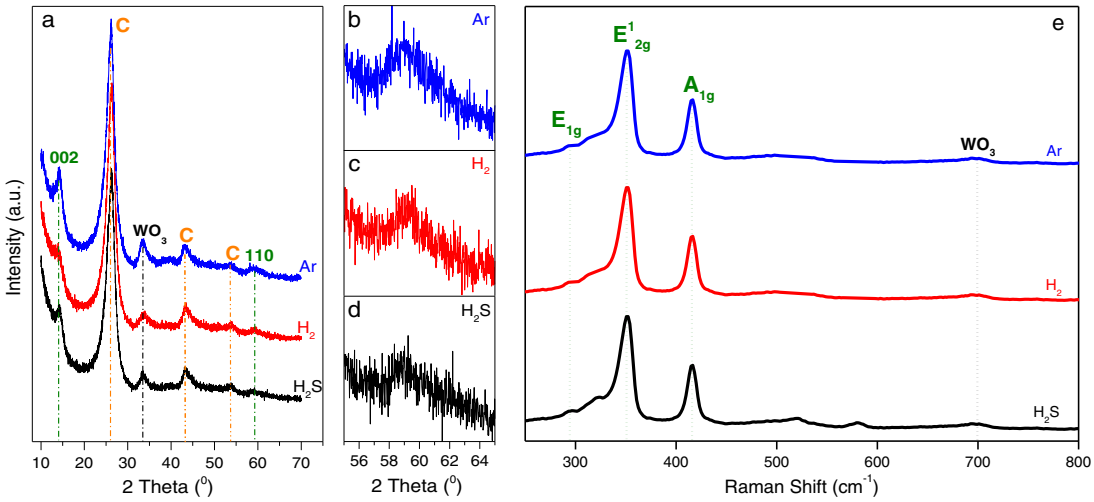

Figure 2. (a) XRD patterns and (b-d) the enlarged (110) peaks of WS_2 (e) Raman spectra for the samples obtained at different gaseous environments. Peaks marked in yellow (C) are from the carbon cloth substrate.

at 160°C to remove the solvent. The baking was performed in air, and the incorporation of oxygen species is expected. Increasing the temperature from 200°C to 800°C leads to the decrease in the intensity of the two W $4f_{7/2}$ components at 33.5 eV and 36.1 eV corresponding to WS_xO_y and WO_3, respectively, indicative of the conversion of tungsten oxy-sulfides and tungsten oxides to tungsten sulfides. The effect of annealing was confirmed from the S 2p core level spectra where the intensity of S $2p_{3/2}$ component at 163.5–163.7 eV attributed to the combination of disulfide pairs S_2^{2-} in WS_xO_y and and/or to bridging disulfide ligands S_2^{2-} and apical S^{2-} from WS_3 decreases as function of the temperature. However, at 400°C the W 4f core level shows the removal of most of WS_xO_y. In contrast, the intensity of

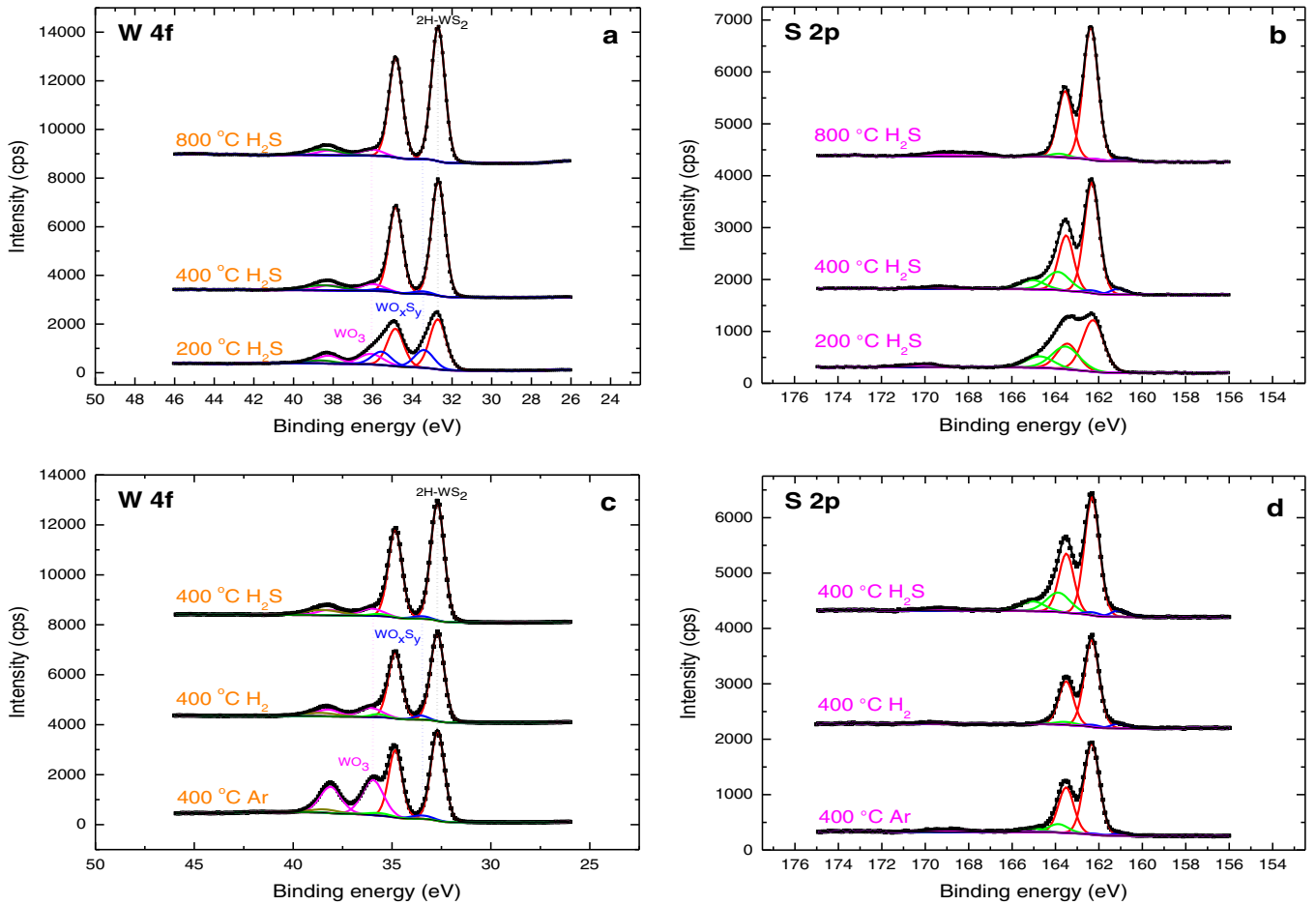

Figure 3. XPS analysis of W 4f and S 2p core levels. (a, b) for samples annealed at different temperatures 200°C, 400°C and 800°C in the presence of H_2S gas. (c, d) for samples annealed at 400°C in the presence of different gases H_2S, H_2 and Ar.

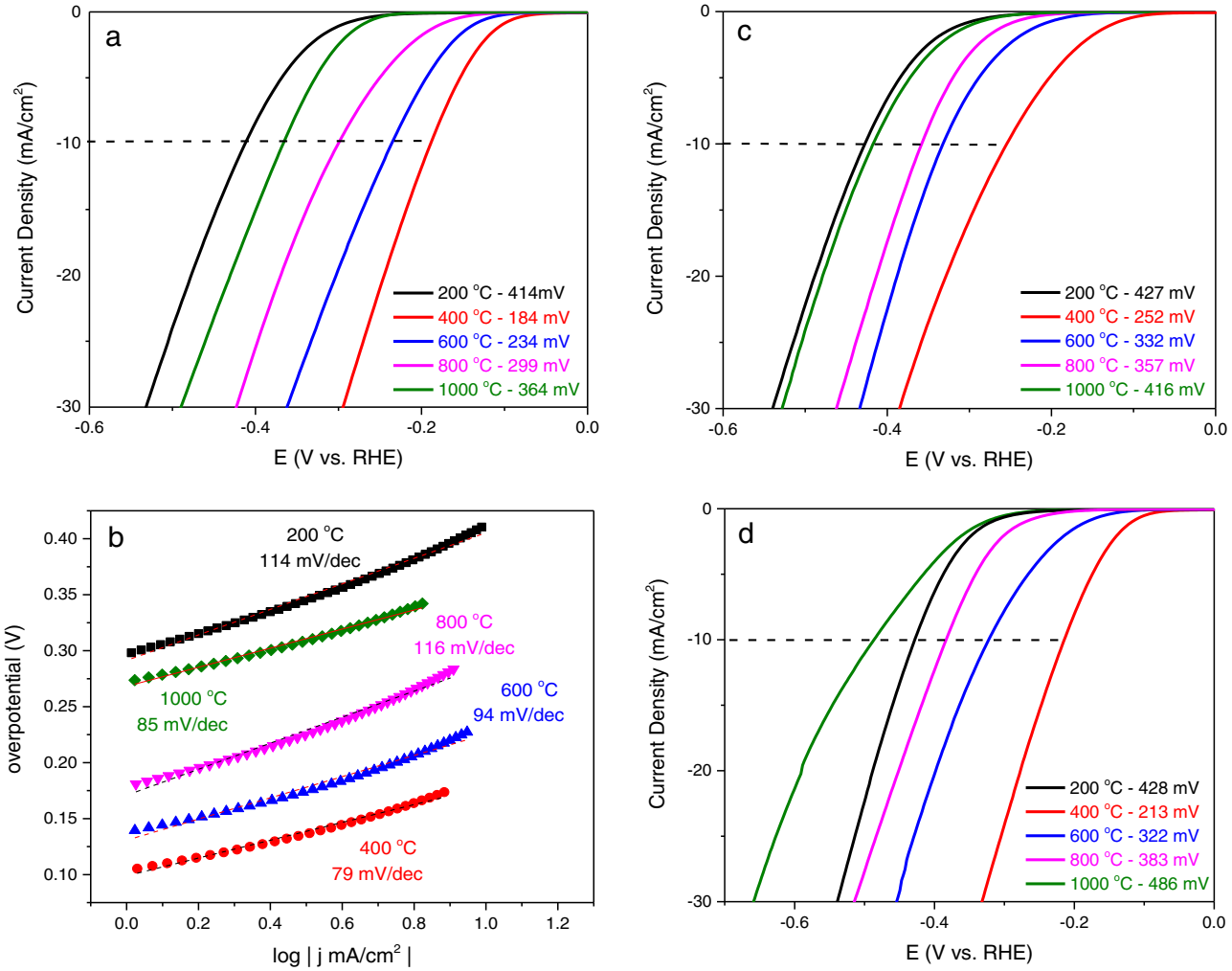

Figure 4. Polarization Curves at a scan rate of 5 mV s^{-1} in 0.5 M H_2SO_4 electrolyte for WS_2 on carbon clothe annealed at different thermolysis temperature. The current was normalized by the geometrical area of the carbon cloth substrate, and the potential was measured after internal resistance correction. (a) 10% H_2S / 90% Ar (c) 10% H_2 / 90% Ar (d) 100% Ar (b) Tafel Slopes extracted from the polarization curves in (a).

S $2p_{3/2}$ component at 163.5–163.7 eV is still pronounced. We conclude that the S $2p_{3/2}$ component at 163.5–163.7 eV at 400°C is mainly due to the bridging disulfide ligands S_2^{2-} and apical S^{2-} from WS_3. The S/W atomic ratio was further estimated from the integrated S 2p and W 4f core level peak area divided by their appropriate relative sensitivity factors. The S/W atomic ratio was equal to 2.06, 2.24 and 2.00 at 200°C, 400°C, and 800°C, respectively. Note that the 200°C-teated sample does not show consistent trend due to the incomplete conversion of structural conversion from precursors as well as the presence of pronounced to WS_xO_y and WO_3.

We notice that at 400°C, the sample was determined to possess composition of $WS_{2.24}$ indicating that the surface of the sample became sulfur rich and confirmed the formation of WS_3 phase. The sample surface structure at 400°C resembles chain-like assemblies of W atoms interconnected by S_2^{2-} or S^{2-} ligands with weak van der Waals interactions between W and S of adjacent chains.[21] From 400°C to 800°C, decomposition of WS_3 occurred and crystalline WS_2 was formed. This was confirmed by the removal of almost all bridging disulfide ligands S_2^{2-} and apical S^{2-} observed at 163.5–163.7 eV and by the S/W atomic ratio which became equal to 2.00.

Moreover, high resolution XPS spectra for the WS_2 samples annealed at 400°C in the presence of different gases Ar, H_2 and H_2S were obtained (Figures 3c and 3d). The same deconvolution parameters were applied. One can notice that in the Ar environment, the presence of strong WO_3 phase (W $4f_{7/2}$ component at 36.1 eV) indicates that the sample was oxidized. In the H_2 environment, however, the sample presents less oxide phase but with the absence of bridging disulfide ligands S_2^{2-} and apical S^{2-} observed at 163.5–163.7 eV for S $2p_{3/2}$. In the H_2S environment at 400°C, the sample is the least oxidized and shows the strongest signal attributed to the bridging disulfide ligands S_2^{2-} and apical S^{2-} from WS_3. It has been well documented that the bridging disulfide ligands S_2^{2-} and apical S^{2-} are the key active sites in MoSx catalysts.[1,24,25] Hence, we concluded that the absence of oxide phase and the presence of bridging disulfide ligands S_2^{2-} and apical S^{2-} from WS_3 with a formal charge state of $[W^{4+}(S_2^{2-})(S^{2-})]$ leads to the best HER performance.

Electrocatalytic Performance for HER

Figures 4a, 4c, and 4d demonstrate the linear sweep voltammetry (LSV) curves of WS_2 on carbon cloth annealed at different thermolysis temperatures and various gas environments with a fixed loading amount of $(NH_4)_2WS_4$ precursor (1 mg cm^{-2}). The HER current density was standardized by the projected area of the carbon cloth, and the potential was measured after correction of internal resistance. We observed that starting from 400°C, the HER performance of annealed WS_2 on carbon cloth is decreasing dramatically as the temperature increases, suggesting that the crystallinity of WS_2 is not playing the key role for HER efficiency.

Figure 4a displays the effect of dihydrogen sulfide gas on the annealed WS_2/CC samples. It is clearly shown that in a variety of some selected temperatures ranging between 200°C–1000°C, the effectiveness of hydrogen evolution increases rapidly from 200°C to 400°C, then decreases in a consistent trend as the temperature goes beyond 400°C. The effect of hydrogen, and argon gases were also examined in this study (Figures 4c and 4d).

Comparing three different gaseous environments and various thermolysis temperatures, annealed sample at 400°C in the hydrogen disulfide gas has been determined as the best performing catalyst with overpotential (vs. RHE) of $\eta_{10} = 184$ mV, because of the sulfur rich surfaces generated from the bridging disulfide ligands S_2^{2-} and apical S^{2-} from WS_3 as discovered by XPS analysis. As above-mentioned, the thermolysis process was carried out at the atmospheric pressure (AP) in a tube furnace, after being pumped and purged with Ar gas aiming to exclude the oxygen species and to minimize the formation of tungsten oxide (WO_3) nanoparticles on the surface of the electrode. As has been reported previously, the HER efficiency of WO_3 is lower than WS_2 structure and it is not the dominating species for HER.[1]

Tafel slopes were extracted from the polarization curves of the catalyst annealed at five different temperatures and saturated with dihydrogen sulfide (Figure 4b). Primarily, as the overpotential increases, a relative small Tafel slope points to a faster hydrogen evolution rate.[26] The Tafel slope of pristine carbon cloth substrate is 185 mV dec^{-1}. When loaded with $(NH_4)_2WS_4$ precursor and annealed at atmospheric pressure, lower Tafel slopes can be observed. In the case of hydrogen disulfide environment, the Tafel slopes of 114 mV dec^{-1}, 79 mV dec^{-1}, 94 mV dec^{-1}, 116 mV dec^{-1}, and 85 mV dec^{-1} were explored for different calcination temperatures of 200°C, 400°C, 600°C, 800°C and 1000°C, respectively. The Tafel slope of WS_2/CC annealed at 400°C in H_2S environment showed the highest performance for the hydrogen evolution.

Conclusions

In summary, tungsten disulfide (WS_2) was successfully prepared by one-step thermolysis process, and the effect of gaseous environments at different temperatures was studied in details. It is found that H_2S gas can strongly affect the amorphous structure of WS_2 and enhance the electrocatalytic performances toward HER behavior. We believe this is an efficient and simple route to obtain highly efficient and cheap electrocatalysts for HER.

Acknowledgments

We thank King Abdullah University of Science and Technology (KAUST) for generous financial support.

References

1. T. Y. Chen, Y. H. Chang, C. L. Hsu, K. H. Wei, C. Y. Chiang, and L. J. Li, *Int. J. Hydrog. Energy*, **38**, 12302 (2013).
2. J. Greeley, T. F. Jaramillo, J. Bonde, I. B. Chorkendorff, and J. K. Norskov, *Nat. Mater.*, **5**, 909 (2006).
3. B. Seger, A. B. Laursen, P. C. K. Vesborg, T. Pedersen, O. Hansen, S. Dahl, and I. Chorkendorff, *Angew. Chem. Int. Ed.*, **51**, 9128 (2012).
4. D. Voiry, H. Yamaguchi, J. W. Li, R. Silva, D. C. B. Alves, T. Fujita, M. W. Chen, T. Asefa, V. B. Shenoy, G. Eda, and M. Chhowalla, *Nat. Mat.*, **12**, 850 (2013).
5. L. Cheng, W. J. Huang, Q. F. Gong, C. H. Liu, Z. Liu, Y. G. Li, and H. J. Dai, *Angew. Chem. Int. Ed.*, **53**, 7860 (2014).
6. A. Sobczynski, A. Yildiz, A. J. Bard, A. Campion, M. A. Fox, T. Mallouk, S. E. Webber, and J. M. White, *J. Phys. Chem.*, **92**, 2311 (1988).
7. A. Sobczynski, A. J. Bard, A. Campion, M. A. Fox, T. E. Mallouk, S. E. Webber, and J. M. White, *J. Phys. Chem.*, **93**, 401 (1989).
8. C. Choi, J. Feng, Y. G. Li, J. Wu, A. Zak, R. Tenne, and H. J. Dai, *Nano Res.*, **6**, 921 (2013).
9. J. Bonde, P. G. Moses, T. F. Jaramillo, J. K. Norskov, and I. Chorkendorff, *Faraday Disc.*, **140**, 219 (2008).
10. Z. Y. Lei, S. J. Xu, and P. Y. Wu, *Phys. Chem. Chem. Phys.*, **18**, 70 (2016).
11. J. Yang, D. Voiry, S. J. Ahn, D. Kang, A. Y. Kim, M. Chhowalla, and H. S. Shin, *Angew. Chem. Int. Ed.*, **52**, 13751 (2013).
12. Y. Mori, M. Tanemura, and S. Tanemura, *Appl. Surf. Sci.*, **228**, 292 (2004).
13. M. O'Brien, K. Lee, R. Morrish, N. C. Berner, N. McEvoy, C. A. Wolden, and G. S. Duesberg, *Chem. Phys. Lett.*, **615**, 6 (2014).
14. T. A. J. Loh, D. H. C. Chua, and A. T. S. Wee, *Sci. Rep.*, **5**, 18116 (2015).
15. I. Martin-Litas, P. Vinatier, A. Levasseur, and J. C. Dupin, *Thin Solid Films*, **416**, 1 (2002).
16. J. C. Dupin, D. Gonbeau, I. Martin-Litas, P. Vinatier, and A. Levasseur, *Appl. Surf. Sci.*, **173**, 140 (2001).
17. Y. Yan, B. Y. Xia, N. Li, Z. C. Xu, A. Fisher, and X. Wang, *J. Mater. Chem. A*, **3**, 131 (2015).
18. T. Alphazan, A. Bonduelle-Skrzypczak, C. Legens, A. S. Gay, Z. Boudene, M. Girleanu, O. Ersen, C. Coperet, and P. Raybaud, *ACS Catal.*, **4**, 4320 (2014).
19. A. J. van der Vlies, G. Kishan, J. W. Niemantsverdriet, R. Prins, and T. Weber, *J. Phys. Chem. B*, **106**, 3449 (2002).
20. T. A. J. Loh and D. H. C. Chua, *J. Phys. Chem. C*, **119**, 27496 (2015).
21. S. M. Tan and M. Pumera, *ACS Appl. Mater. & Interf.*, **8**, 3948 (2016).
22. K. S. Liang, S. P. Cramer, D. C. Johnston, C. H. Chang, A. J. Jacobson, J. P. Deneufville, and R. R. Chianelli, *J. Non-Crystalline Solids*, **42**, 345 (1980).
23. D. Meissner, C. Benndorf, and R. Memming, *Appl. Surf. Sci.*, **27**, 423 (1987).
24. Y.-H. Chang, C.-T. Lin, T.-Y. Chen, C.-L. Hsu, Y.-H. Lee, W. Zhang, K.-H. Wei, and L.-J. Li, *Adv Mater.*, **25**, 756 (2013).
25. H. Vrubel, D. Merki, and X. Hu, *Energy Environ. Sci.*, **5**, 6136 (2012).
26. L. Tao, X. D. Duan, C. Wang, X. F. Duan, and S. Y. Wang, *Chem. Commun.*, **51**, 7470 (2015).